THE BREAKING OF A SINGLE ASPERITY: ANALYSIS OF AN AFTERSHOCK OF THE 1975 OROVILLE, CALIFORNIA, EARTHQUAKE

S. Das (I)
J. Boatwright (II)
Presenting Author: S. Das

SUMMARY

We have modelled acceleration envelopes from a small aftershock with the objective of understanding the character of the acceleration radiated by the failure of a single, isolated asperity on a fault plane. The most prominent characteristics that we model are a prolonged emergent onset followed by a strong pulse. We interpret this energetic radiation to occur at the completion of failure of the asperity.

INTRODUCTION

Seismic information on the details of the faulting process is contained in body waves whose periods are short compared to the overall duration of faulting. Because velocity and displacement spectra are peaked at the corner period and fall off at shorter periods, it is necessary to consider the radiated acceleration field to appropriately analyze this period range. In general, the radiated accelerations are incoherent and difficult to interpret uniquely. The fracture process in large earthquakes contains many different source areas radiating simultaneously. To analyze these earthquakes requires low-pass filters for both the data and the model in order to restrict the number of free parameters. Unfortunately, such filtering tends to obscure the spatial and temporal details of the stress release, in which we are interested.

In contrast, analyzing relatively small events can provide a useful test for theories of the faulting process. Such an approach was taken by Boatwright (Ref. 1) using a quasi-dynamical model of rupture. Even for small events, however, the enormous parameter requirements (defining the stress and strength over the fault surface) usually prohibit a fully dynamical modeling of the earthquake. In this paper, we use the results of a forward dynamic problem to interpret the mechanics of an observed earthquake source. The theoretical accelerogram envelopes generated by the failure of a circular asperity are compared with the envelopes of the accelerograms written by a small (M_L = 3.6) aftershock of the 1975 Oroville, California, earthquake.

(I) Lamont-Doherty Geological Observatory of Columbia University, Palisades, New York USA

(II) U.S. Geological Survey, 345 Middlefield Road, Menlo Park, California USA

THEORETICAL MODEL

Das and Kostrov (Ref. 2) studied the fracture process and the wave field radiated by the dynamic failure of a circular asperity. The asperity was surrounded by an infinite broken fault plane with a constant displacement applied at infinity. In their model, once the asperity failed at a point, the rupture propagated first around the perimenter where the stress was most strongly concentrated and then ruptured the interior. The authors referred to this rupture geometry as a "double encircling pincer movement". The fracture process for one of the cases studied by the authors is shown in Figure 1a. The far-field displacement waveform radiated by this failure in the direction along the normal to the fault plane is shown in Figure 1b and the corresponding acceleration is shown in Figure 1c. The failure of the last point of the asperity is the most energetic part of the fracture process and radiates the strongest acceleration pulse. Note that the displacement waveform does not return to zero after the failure of the asperity is completed, but stays at the same constant level, as a result of the equilibration of slip in the region surrounding the asperity. The radiated displacement waveforms depend primarily on the clustering of the grid points and less on the number of grid points which fail at a given time-step. This distinction is not true, however, for the radiated accelerations. The acceleration radiated in the direction along the normal to the fault at a given time-step depends only on the number of grid points which fail at that time-step and is independent of the clustering of the grid points.

An assumption of this model limits its applicability. The stress on the (infinite) fault plane surrounding the asperity is initially at the dynamic frictional level and remains unchanged throughout the breaking of the asperity. In simple terms, the fault plane surrounding the asperity is assumed to have no strength which results in the displacement waveform continuing at a constant non-zero level so that the fact that no acceleration is radiated after completion of breaking of the asperity result from this feature of the model. This assumption permits a significant reduction in computer time required to run the model, but is clearly unrealistic for any actual seismic rupture, where the previously broken area around an asperity is necessarily finite, and even if the previous rupture is relatively recent, the fault plane can be assumed to have regained some strength (Ref. 3). Because of these limitations, the model used here is valid only up to the time of the complete failure of the asperity and should only be used to analyze the rise of the radiated displacement pulse (Ref. 2).

EVENT J

The accelerations generated by the aftershocks of the 1975 Oroville, California, earthquake were recorded by a set of SMA-1's deployed in the three days following the main shock. The epicentral area of the main shock and the northern aftershocks is shown in Figure 2, along with the distribution of the accelerographs. The epicenter of event J is shown darkened. The aftershocks have been extensively studied by Fletcher (Ref. 4) and Boatwright (Refs. 1, 5, 6, 7,). In particular, Boatwright

(Ref. 6) estimated the rupture areas of the eight best recorded aftershocks, including event J, which we will analyze in this paper. The distribution of hypocenters and rupture areas of the events which occurred up to and including event J are shown in Figure 3. Event F, which occurred some 13 hours before event J, was one of the largest events of the aftershock sequence. The inferred rupture area of event F almost entirely surrounds event J. There were no aftershocks of event J. On the basis of these locations and the estimated rupture geometries, the conditions on the fault area surrounding event J are as close as possible to the boundary conditions of the Das and Kostrov (Ref. 2) model. This provided the motivation for analyzing this event using the asperity model.

Figure 4a shows an upper hemisphere plot of the fault plane solution for Event J; Figure 4b shows the takeoff angles with respect to the fault plane (obtained by rotating Figure 4a so that the fault plane coincides with the plane of the stereonet). For this event, most of the takeoff angles of the recorded S-waves are near the direction of the normal to the fault plane.

COMPARISON OF SYNTHETIC AND OBSERVED ACCELERATION ENVELOPES

We have computed the complex envelopes of the accelerations using the definition of Farnbach (Ref. 8),

$$u^*(t) = (1/2)\sqrt{u^2(t) + H^2[u(t)]}$$

where H[ ] denotes the Hilbert transform. Note that this definition conserves the power of the complex signal; squaring both sides of the equation above and integrating over time gives

$$\int [u^*(t)]^2 dt = \int u^2(t) dt.$$

Because the phase information is removed from the accelerations by this operation, it is possible to combine the two horizontal components to obtain a single trace which contains all the power of the horizontal accelerations. Figure 5 demonstrates the calculation of the acceleration envelope for one horizontal component for station 3. In Figure 6, we compare the synthetic envelopes to the total horizontal envelopes. The most prominent feature of the envelopes of the observed accelerations is the dominant peak which appears on all six stations studied here. The emergent part of the synthetic envelopes only qualitatively agrees with the total horizontal envelopes while the dominant pulse is well modelled.

Finally, the absolute scaling of the synthetics to the total horizontal envelopes can be used to determine an estimate of the average dynamic stress drop of the asperity. Table I shows the hypocentral distance R and peak acceleration recorded at the six stations. From Das and Kostrov (Ref. 2), the average stress drop on the circular asperity is

$$\sigma_{13}(r) = \frac{32}{7\pi} \frac{\mu u_o}{r_o}$$

where u_o is the applied displacement at infinity and r_o is the radius of the asperity, taken as 42 m (Ref. 7). The synthetic far-field displacements are given by the equation

$$u_n^S(x,t) = (\text{S-directivity function}) \frac{1}{4\pi\rho\beta^2 R} \iint \tau_{13}\left(\xi, t-\frac{R-\xi\cdot\gamma}{\beta}\right) dS(\xi)$$

Taking β = 3.5 km/sec, ρ = 3 gm/cm^3, μ = 4x10^{11} dyne/cm^2, and adjusting for the radiation pattern and a free surface amplification factor of 2 gives an average dynamic stress drop of $\approx$ 250 bars. In comparison, the stress drops obtained for this event by Boawright (Ref. 7) and Fletcher et. al. (Ref. 4) range from 30 bars to 140 bars. These methods of analysis do notaccount for the asperity mode of rupture, however. The stress drops calculated for event F ranged from 170 to 350 bars (Ref. 4, 7). In particular, the dynamic stress drop was 256 bars. Thus the asperity stress drop appears to correspond to the stress drop of the event which ruptured the fault plane around the asperity.

DISCUSSION

The main point considered here is how the character of the waveforms reflects the character of the rupture process, viz; an emergent, incoherent onset followed by a very energetic acceleration pulse. The emergent beginning is interpreted as reflecting a heterogeneous initial stress distribution rather than a specific geometry of rupture. In the model, the energetic acceleration pulse is radiated as the asperity failure is completed. Because of the relative location of the event within the rupture area of a previous event, the similarity of the synthetic and recorded acceleration envelopes, and the lack of aftershocks, the interpretation of an asperity failure appears reasonable. While the fits to the total horizontal envelopes are good, the rupture geometry used to generate the synthetics cannot be uniquely inferred from the fitting procedure. Specifically, while it is clear from the recorded accelerations that the onset of the rupture process is not particularly energetic, it is impossible to conclude that the rupture is "encircling" the asperity during this phase. In the theoretical model, the exact behavior of the rupture onset is conditioned by the distribution of the initial stress. The "encircling pincers" only follow the initial stress concentration along the perimenter of the asperity. To determine the geometry of such a stress distribution from the recorded pulse shapes requires both a more complete sampling of the focal sphere and a better signal to noise ratio. These details are superfluous, however, to the overall purpose of this analysis.

CONCLUSIONS

We have modelled the acceleration envelopes from a small aftershock to understand the expected characteristics of the acceleration radiated by the failure of an asperity. These characteristics include a prolonged emergent onset of the waveform that precedes a strong pulse in acceleration envelope which is radiated as the failure of the asperity is completed. The continuing acceleration which follows the completion of

the asperity failure cannot be modelled using the results of Das and Kostrov (Ref. 2) which predict continuing displacement during the equilibration of slip outside the asperity. Our interpretation of the continuing acceleration in the observed accelerograms is that the fault area outside the asperity has regained strength in the time between Event F and Event J. The rerupturing of this area will then be accompanied by a small (but finite) stress change which necessarily radiates acceleration but is not modelled here.

TABLE I

Station	Distance R from Focus to Station (km)	Peak Observed Acceleration[1] (cm/sec^2)
DWR	10.1	71.
CD2	14.7	20.
CD5	11.7	62.
CD3	15.4	56.
OAP	12.1	29.
EBH	11.1	32.

[1] Accelerograms not included in paper

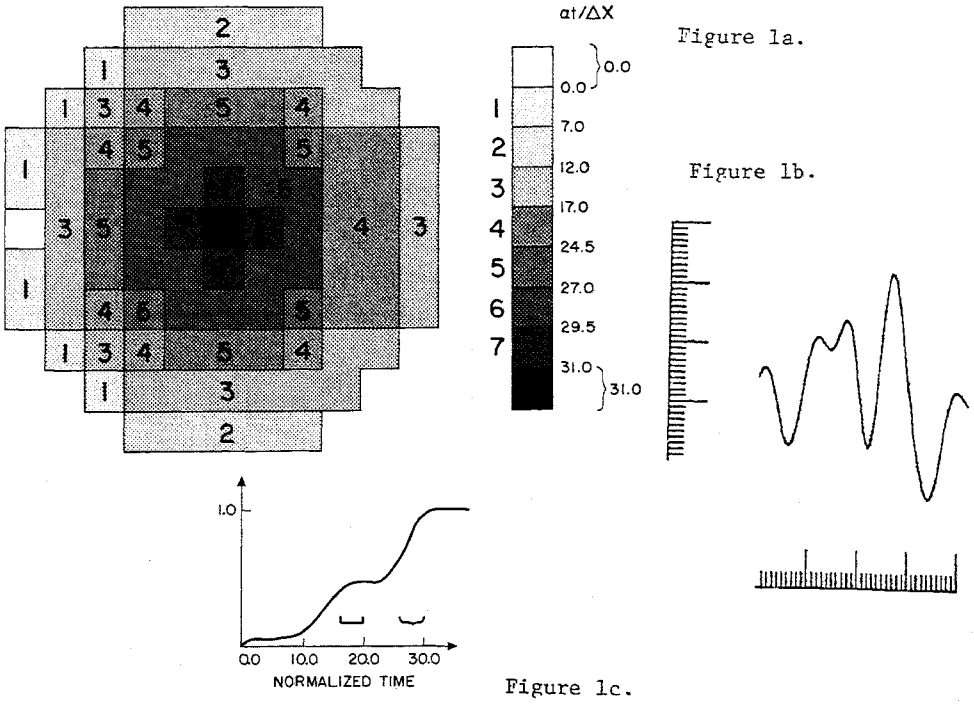

Figure 1a.

Figure 1b.

Figure 1c.

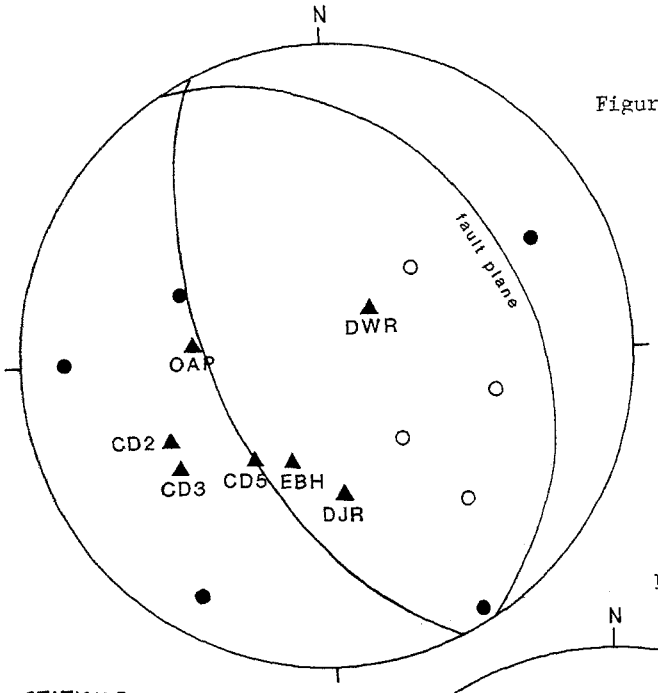

Figure 4a

Figure 4b

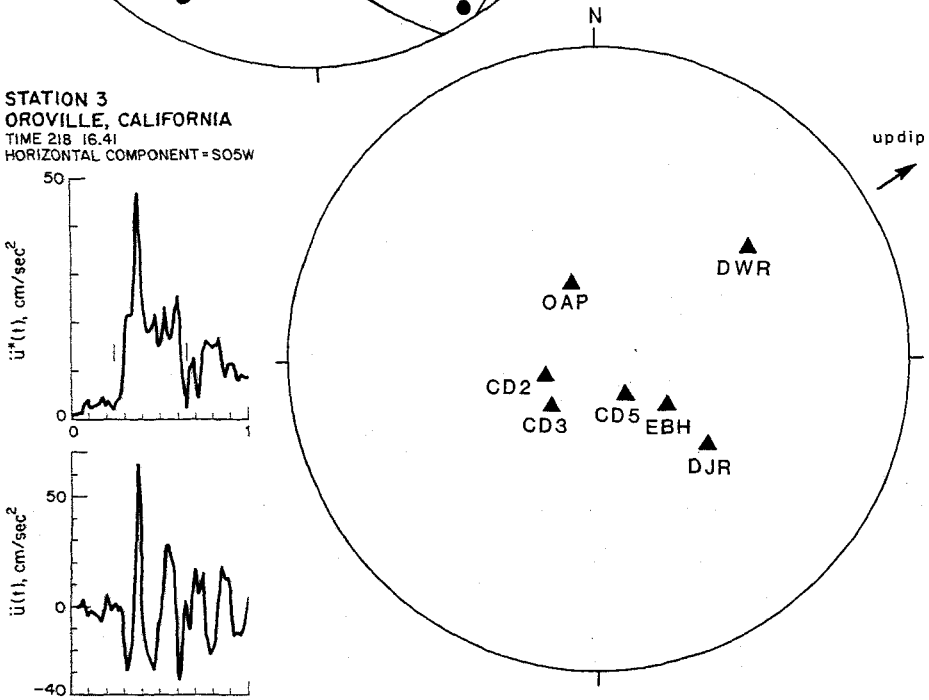

Takeoff Angles wrt Fault Plane

Figure 5

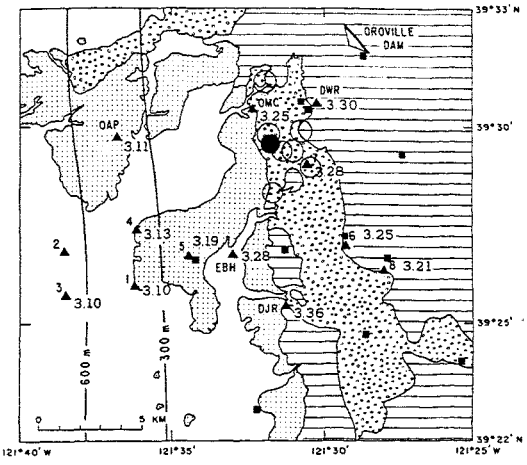

Figure 2

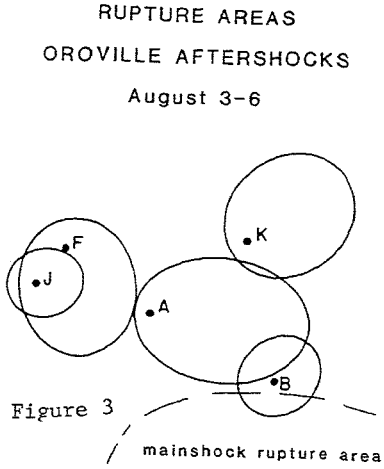

Figure 3

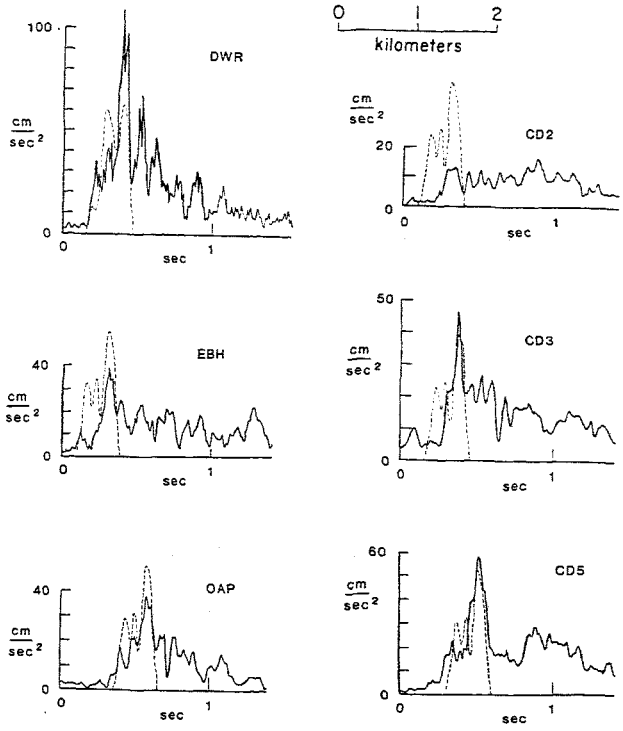

Figure 6

Figure Captions

Figure 1a. Broken areas as a function of time for the case named Case II, after Das and Kostrov (Ref. 2). The key indicates the areas broken during the normalized time intervals marked.

Figure 1b. Normalized "far-field" S-displacement pulse shape, looking vertically down at the fault.

Figure 1c. Filtered S-acceleration due to displacement pulse shown in Figure 1b.

Figure 2. Epicentral region of the Oroville, California earthquake showing strong-motion accelerogram sites (triangles). The open circles show the nothern aftershock epicenters. Event J is shown by a solid circle.

Figure 3. Geometry of the broken areas for some Oroville aftershocks, after Boatwright (Ref. 7). Note that event F occurred prior to event J.

Figure 4a. Upper hemisphere plot of fault-plane solution for event J.

Figure 4b. Plot showing the stations plotted back onto the broken area of event J to indicate from which point of the fault the first radiation arrives at the station.

Figure 5. One horizontal component of the accelerogram at station 3 at Oroville due to event J and its complex envelope, to demonstrate the advantages of using the envelope rather than the original time signal.

Figure 6. Comparison of the complex envelopes of the observed solid lines and theoretical accelerations (dotted lines). Note that we only compare shapes in this figure and no correction has (yet) been made for distance and radiation patterns.

REFERENCES

1) Boatwright, J.L., (1981). Quasi-dynamical models of simple earthquakes; application to an aftershock of the 1975 Oroville, Clalifornia earthquake, Bull. Seismol. Soc. Am., 71, 69-94.

2) Das, S., and B.V. Kostrov, (1983). Breaking of a single asperity: Rupture process and seismic radiation, J. Geophys. Res., 88(B5), 4277-4288.

3) Dieterich, J.H., (1979). Modelling of rock friction: I. Experimental Results and Constitutive Equations, J. Geophys. Res., 84, 2161-2168.

4) Fletcher, J.B., A.G. Brady, and T.C. Hanks, (1980). Strong-motion accelerograms of the Oroville, California, aftershocks: Data processing and the aftershock of 0350 August 6, 1975, Bull. Seismol. Soc. Am., 70(1), 243-267.

5) Boatwright, J.L., (1980). A spectral theory for the circular seismic sources; simple estimates of source dimension, dynamic stress-drop and radiated seismic energy, Bull. Seismol. Soc. Am., 70, 1-27.

6) Boatwright, J.L., (1983). Seismic estimates of stress release, J. Geophys. Res., in press.

7) Boatwright J.L., (1984). The effect of rupture complexity on estimates of source size, submitted to Bull. Seismol. Soc. Am.

8) Farnbach, J.S., (1975). The complex envelope in seismic signal analysis, Bull. Seismol. Soc. Am, 65,(4), 951-962.